Cumhuriyet Science Journal
CSJ

e-ISSN: 2587-246X
ISSN: 2587-2680

Cumhuriyet Sci. J., Vol.39-1(2018) 144-151

# Application of Spectroscopic Methods for Analysis of Ni-Based Alloys (Ni% ≥70)

***Zeynep AYGUN***

*Bitlis Eren University, Vocational School of Technical Sciences, 13000, Bitlis, TURKEY*

Received: 05.07.2017; Accepted: 12.03.2018 *http://dx.doi.org/10.17776/csj.405681*

**Abstract:** In this paper, we investigate the structural and magnetic properties of Ni based alloys which are in the form of $Ni_xFe_yMo_z$ (x = 0.80; y = 0.15; z = 0.05), $Ni_xCr_yFe_z$ (x = 0.70; y = 0.20; z = 0.10), and $Ni_xCr_yAl_zCu_t$ (x = 0.75; y = 0.20; z = 0.025; t = 0.025) and are prepared by heating the pellet formed samples at high temperature. For this purpose, electron paramagnetic resonance experiment is performed for analysis of paramagnetic centers of these compositions to see the behaviours of alloys in an external magnetic field. g values are calculated from electron paramagnetic resonance spectra recorded at room temperature. Structural features of $Ni_xFe_yMo_z$, $Ni_xCr_yFe_z$ and $Ni_xCr_yAl_zCu_t$ alloys are observed by x-ray diffraction technique. Line positions and line intensities are discussed by the help of x-ray diffraction spectra recorded at room temperature. In order to understand the surface morphology of samples, scanning electron microscopy; for the elemental compositions of the alloys energy dispersive spectrosopy experiments are carried out at room temperature.

***Keywords*:** Ni-based alloys, magnetic properties, structural features

# Ni-Esaslı Alaşımların (Ni% ≥70) Analizi için Spektroskopik Yöntemlerin Uygulanması

**Özet:** Bu çalışmada $Ni_xFe_yMo_z$ (x = 0.80; y = 0.15; z = 0.05), $Ni_xCr_yFe_z$ (x = 0.70; y = 0.20; z = 0.10), and $Ni_xCr_yAl_zCu_t$ (x = 0.75; y = 0.20; z = 0.025; t = 0.025) şeklinde olan ve yüksek sıcaklıklarda pellet formunda ısıtılarak hazırlanan Ni esaslı alaşımların yapısal ve manyetik özellikleri incelenmiştir. Bu amaçla, dış manyetik alanda alaşımların davranışlarını görmek için bu kompozisyonların paramanyetik özelliklerinin analizinde elektron paramanyetik rezonans deneyi kullanılmıştır. Oda sıcaklığında kaydedilen elektron paramanyetik rezonans spektrumlarından g değerleri hesaplanmıştır. $Ni_xFe_yMo_z$, $Ni_xCr_yFe_z$ and $Ni_xCr_yAl_zCu_t$ alaşımlarının yapısal özellikleri x-ışını kırınımı tekniği ile gözlemlenmiştir. Çizgi yerleri ve şiddetleri oda sıcaklığında kaydedilen x-ışını kırınımı spektrumları ile tartışılmıştır. Numunelerin yüzey morfolojisini anlamak için taramalı elektron mikroskobu; alaşımların elementel kompozisyonu için enerji dağılımlı spektroskopi deneyleri oda sıcaklığında yürütülmüştür.

***Anahtar Kelimeler*:** Ni-esaslı alaşımlar, manyetik özellikler, yapısal özellikler

## 1. INTRODUCTION

The material obtained by processing two or more metals together in various proportions with different methods can be designated as alloy. For the development of modern technology, the 3d transition metals and their alloys have had great interest and have played an effective role due to their investigated physical parameters for different applications. Results obtained by the formation of alloys may reduce cost of material

* Corresponding author. *Email address:* *zeynep.yarbasi@gmail.com, zaygun@beu.edu.tr*

while preserving or changing some important properties of the component of alloys. Hence, they are used in a wide variety of applications. In this context, alloys with different ingredients and obtained by different methods have taken part in many studies before [1-3]. Among these many alloys, Ni-based alloys consist of nickel as main solute with at least 50% content, have great interest because of preferring in different areas such as aerospace engines, marine equipment, nuclear reactors, and petrochemical industries [4]. 79% Ni, 16% Fe, and 5% Mo composition is known as a soft magnetic material and is characterized by high permeability and low coercivity. The high-nickel based alloys containing about 79% Ni have high initial and maximum permeabilities and very low hysteresis losses; additions of 4 to 5% Mo, or of copper and chromium to 79Ni-Fe alloys, brings to the fore the magnetic characteristics [5]. Therefore, it is important to study the magnetic features of Ni based alloys due to their uses in different applications and various important properties.

In the present work, our aim is to observe the magnetic properties in an external magnetic field and structural features of Ni-based alloys consist of $Ni_xFe_yMo_z$ (x = 0.80; y = 0.15; z = 0.05), $Ni_xCr_yFe_z$ (x = 0.70; y = 0.20; z = 0.10) and $Ni_xCr_yAl_zCu_t$ (x = 0.75; y = 0.20; z = 0.025; t = 0.025). Therefore, electron paramagnetic resonance (EPR), a spectroscopic technique that helps us to recognize quantum systems with unpaired electron by using the microwave region of the electromagnetic spectrum, is preferred to determine the paramagnetic centers of the structure. EPR spectroscopy is interested in the spin transitions between the energy states in the presence of an external magnetic field, while they are degenerate in the absence of magnetic field [6]. In addition, we perform X-ray diffraction (XRD) study to make qualitative analysis of alloys $Ni_xFe_yMo_z$, $Ni_xCr_yFe_z$ and $Ni_xCr_yAl_zCu_t$. XRD is one of the most preferred techniques to obtain information about the chemical composition and crystallographic structure of any crystalline material. While XRD pattern of NiFeMo alloy was given by Wang *et al.* [7], the method used for preparing the sample and also the proportions of elements were different from our study. In order to have knowledge in detail for determining near surface properties of samples, SEM (scanning electron microscopy) is used. With SEM technique, another system EDS (energy dispersive spectrosopy) is used. A point, line and area scan, selected areas X-ray mapping, qualitative and quantitative analyzes in these areas can be determined by EDS system.

In the previous studies, NiFeMo alloy were reported by different sample preparation and different analysis methods [8,9]. However, to the best of our knowledge, there are no EPR, XRD, SEM and EDS studies about $Ni_{0.80}Fe_{0.15}Mo_{0.05}$, $Ni_{0.70}Cr_{0.20}Fe_{0.10}$ and $Ni_{0.75}Cr_{0.20}Al_{0.025}Cu_{0.025}$ alloys in the literature. Thus, having magnetic and structural information for these compositions with given element rates will be helpful to address this lack.

## 2. EXPERIMENTAL

### 2.1. Sample Preparation

In our studies, we prefer two sample forms for alloys. One of these is to prepare the alloys by providing total concentration one with pure 3d transition metals which are bought commercially in powder form. They are milled by using agate hand-mortar and are stirred in the sample mixer to obtain a homogeneous dispersion. Thus, particle size and absorption effects are minimized within the possibilities. These mixtures are pressed under pressure for making pellets. Prepared pellets are heated at high temperatures for having alloys. The second way is to order these samples in the foil form commercially. In this study, we have supplied our alloys in foil form from Goodfellow Corporation in the size of 0.012 mm thickness; 10 mm diameter for $Ni_{0.8}Fe_{0.15}Mo_{0.05}$, 0.025 mm thickness; 15 mm diameter for $Ni_{0.70}Cr_{0.20}Fe_{0.10}$ and 0.025 mm thickness; 10 mm diameter for $Ni_{0.75}Cr_{0.20}Al_{0.025}Cu_{0.025}$.

### 2.2. Instrumentation

An X-band JEOL JESFA-300 EPR spectrometer with 100 *kHz* modulation field and 9.23 *GHz* frequency was used for recording EPR spectra at room temperature. Diamagnetic tubes were used for samples in the pellet form performing by EPR spectrometer.

The XRD patterns of alloy samples were obtained using JEOL D8 ADVANCE XRD, which was operated at 40 kV and 40 mA with a scanning speed of 2.5˚ $min^{-1}$. Cu Kα radiation of wavelength $\lambda$ = 1.54059 Å was used and data was taken for the $2\theta$ range of 3˚ – 90˚.

In SEM technique, an electron gun with thermoionic emision is usually used for producing electron. Obtained electrons are accelerated in high voltage (1 – 30 keV) and condenser lenses are used to demagnify electron beam until it has a diameter of approximately 10 nm. The signals composed due to the interaction between incident electron beam and sample give us different information about the specimen. The scanning electron microscope images of powders were measured by JEOL JSM-6610 SEM Spectrometer.

## 3. RESULTS and DISCUSSION

### 3.1. EPR measurements

The observed EPR signals are identified by *g*-values and these values are calculated from the equation $h\upsilon = g\beta H$ with $H$ the magnetic field, $\upsilon$ the microwave frequency, $h$ the Planck constant and $\beta$ the electron Bohr magneton. $g$ is an unitless constant which is a distinctive property of studied sample. EPR spectra of $Ni_{0.80}Fe_{0.15}Mo_{0.05}$ and $Ni_{0.75}Cr_{0.20}Al_{0.025}Cu_{0.025}$ alloys are taken at room temperature and given in Figure 1. For alloy $Ni_{0.80}Fe_{0.15}Mo_{0.05}$, three EPR lines are observed with g values of 5.665, 5.333 and 4.396 centered at 1164 G(Gauss), 1236.5 G and 1500 G, respectively (Figure 1a). All obtained EPR lines are not well-resolved and overlapped, so we are not able to identificate the peaks clearly. As shown in Figure 1b, g values of $Ni_{0.75}Cr_{0.20}Al_{0.025}Cu_{0.025}$ alloy are calculated as 3.719, 2.442 and 2.049. All three lines are broad and this broadness may be due to the dipole-dipole interactions between the interacting spins. EPR spectra of $Ni^{2+}$ ($d^8$) ion are observable generally at low temperatures. At room temperature, very few papers have been seen in the literature and in these reports isotropic g value of Ni was given close to 2.2 value [10]. A g value of 2.343 due to the $Ni^{2+}$ was reported in the previous study [11]. We are awared of from the reports that the g value of 4.396 can be attributed to $Fe^{+3}$ ion [12]. It was reported that the resonance at g ≈ 4.3 corresponds to high-spin isolated $Fe^{+3}$ in the glassy matrix [12]. As we observed from our EPR result (Figure 1b), it was also defined by Reddy *et al.* [13] that the broad resonance signal at g ≈ 2.049 is a characteristic of $Cu^{2+}$ ion. Additionally, we are known that the g values of isotropic $Cu^{2+}$ centers are generally located in the 2.100 - 2.200 range from previous papers [14-16]. Also according to the studies reported before, we are able to label the line with g ≈ 6.0 as hematite ($Fe_2O_3$) [17,18]. For g = 3.719 line, it can be said that this EPR line is due to some iron centers as mentioned in previous studies [19-21]. Also an EPR signal at g = 3.7 value was reported by Davis *et al.* [22] as a FeMo protein signal. Also in the same study, the line given with g ≈ 2.0 was explained as Fe signal [22]. EPR spectrum of $Ni_{0.70}Cr_{0.20}Fe_{0.10}$ alloy is given in Figure 2. The observed EPR lines for $Ni_{0.70}Cr_{0.20}Fe_{0.10}$ have the g values of 2.078, 2.026 and 1.934. Signals with 2.078 and 1.934 values are broad compared to line with g value of 2.026. The broadening of EPR signals can be arisen from the dipole-dipole and exchange interaction between the interacting spins. Kabir *et al.* [15] determined the g values of 1.943 and 1.967 for NiFe alloy and 1.966 for Ni. Fedorov *et al.* [23] reported a g value of ≈ 2.040 for $Fe^{3+}$ close to our result. It was expressed by Vercamer et al. [24] that the signal with g = 2 can be attributed to $Fe^{3+}$ with high symmetry. EPR signal with g value ≈ 1.9 indexed to Cr(III) center was obtained by PusphaManjari *et al.* [25]. Also, Padlyak *et al.* [26] gave the g ≈ 2.020 value for $Cr^{3+}$ (dip). Therefore, it can be concluded that the obtained

g values of EPR signals for our samples are in good agreement with the given literature results. Additionally, paramagnetic features of all studied alloys are dedected by EPR experiments.

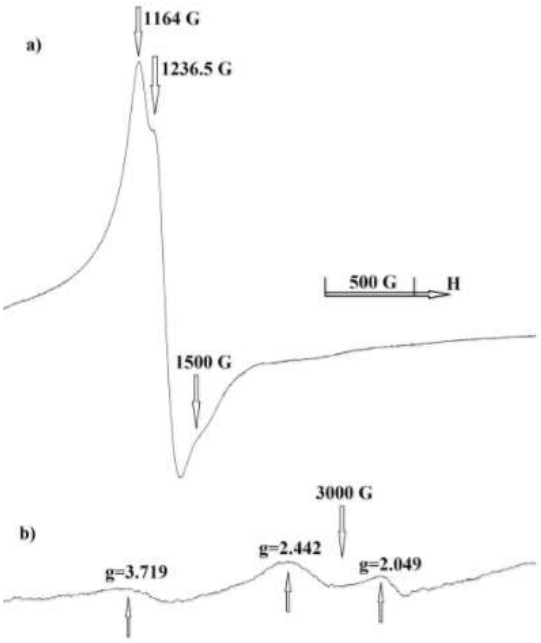


**Figure 1.** EPR spectra of a) $Ni_{0.80}Fe_{0.15}Mo_{0.05}$ and b) $Ni_{0.75}Cr_{0.20}Al_{0.025}Cu_{0.025}$ alloys recorded at room temperature.

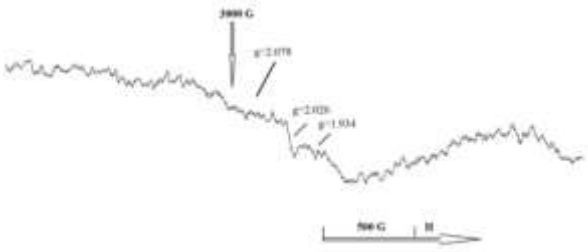

**Figure 2.** EPR spectrum of $Ni_{0.70}Cr_{0.20}Fe_{0.10}$ alloy recorded at room temperature.

### 3.2. XRD measurements

The XRD patterns of $Ni_{0.80}Fe_{0.15}Mo_{0.05}$, $Ni_{0.70}Cr_{0.20}Fe_{0.10}$ and $Ni_{0.75}Cr_{0.20}Al_{0.025}Cu_{0.025}$ alloys are seen in Figure 3. In Figure 3a, sharp peaks centered at $2\theta \approx 44.0^{\circ}$, $51.2^{\circ}$, $51.3^{\circ}$, $75.5^{\circ}$ and $75.7^{\circ}$ are observed for $Ni_{0.80}Fe_{0.15}Mo_{0.05}$ alloy. Peak located at $44.0^{\circ}$ can be assigned as $Fe_2O_3$ which was mentioned also by Aliahmad *et al.* [27]. Other $Fe_2O_3$ peak centered at $\approx 75.0^{\circ}$ was again reported before by Drbohlavova *et al.* [28]. For Iwasaki, this peak with $\approx 75.0^{\circ}$ value might be labeled as $Fe_3O_4$ [29]. Also, XRD peak of $\approx 75.0^{\circ}$ was assigned as Mo [2]. Other Bragg reflections seen at $2\theta \approx 43.9^{\circ}$, $51.0^{\circ}$, $51.1^{\circ}$, $75.2^{\circ}$ and $75.4^{\circ}$ are given for $Ni_{0.75}Cr_{0.20}Al_{0.025}Cu_{0.025}$ alloy in Figure 3b. Ul-Hamid et al. [30] gave the characteristic Ni peak $2\theta \approx 44.0^{\circ}$. Hence, the peak centered at $2\theta \approx 44.0^{\circ}$ and $43.9^{\circ}$ can be attributed to Ni for both of the alloys. The peaks located at $43.9^{\circ}$ and $\approx 75.0^{\circ}$ can be attributed to $Fe_2O_3$ and $Fe_3O_4$ compounds as mentioned and shown in EPR explanations (Figure 3a). XRD peaks centered at $43.9^{\circ}$ and $\approx 51.0^{\circ}$ are observed as Cu peaks [31]. For $Ni_{0.75}Cr_{0.20}Al_{0.025}Cu_{0.025}$ alloy, $43.9^{\circ}$ and $\approx 75.0^{\circ}$ are also obtained as Al peaks [2]. Reflection angles of $Ni_{0.70}Cr_{0.20}Fe_{0.10}$ alloy centered at $2\theta = 43.8^{\circ}$, $51.1^{\circ}$ and $75.3^{\circ}$ are obtained and shown in Figure 3c. For $Ni_{0.70}Cr_{0.20}Fe_{0.10}$ alloy, our observed peaks located at $2\theta = 43.8^{\circ}$, $51.1^{\circ}$ and $75.3^{\circ}$ are in harmony with the values given by Saravanan and Mohan [32]. Additionally, Park *et al.* [33] gave the Cr peak centered at $\approx 44^{\circ}$. The sharpness of peaks are determinative to get information about the crystalline nature of the samples. We can express that the line shapes of XRD patterns show the crystalline phase.

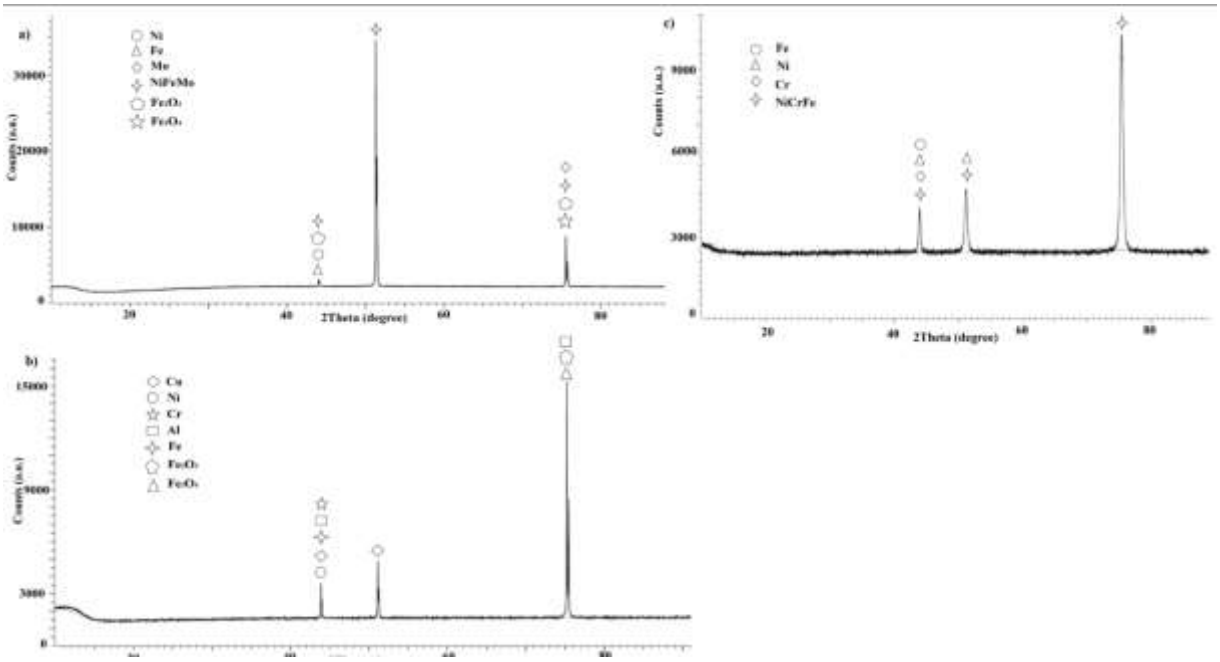

**Figure 3.** XRD patterns of a) $Ni_{0.80}Fe_{0.15}Mo_{0.05}$ b) $Ni_{0.75}Cr_{0.20}Al_{0.025}Cu_{0.025}$ and c) $Ni_{0.70}Cr_{0.20}Fe_{0.10}$ alloys recorded at room temperature.

### 3.3. EDS measurements

EDS measurements are carried out at room temperature to determine the elemental compositions of samples and obtained results are given in Figure 4. As seen in Figure 4, contents of three alloys, Cu, Ni, Cr, Mo Al and Fe, are determined by EDS. The amount of elements are also given. For $Ni_{0.75}Cr_{0.20}Al_{0.025}Cu_{0.025}$ alloy, we could not dedect the Fe elemental weight by EDS, this may be because of the instrumental sensitivity, less than 0.1% can not be detected by EDS, while some ferric centers are seen by XRD and EPR methods for this alloy.

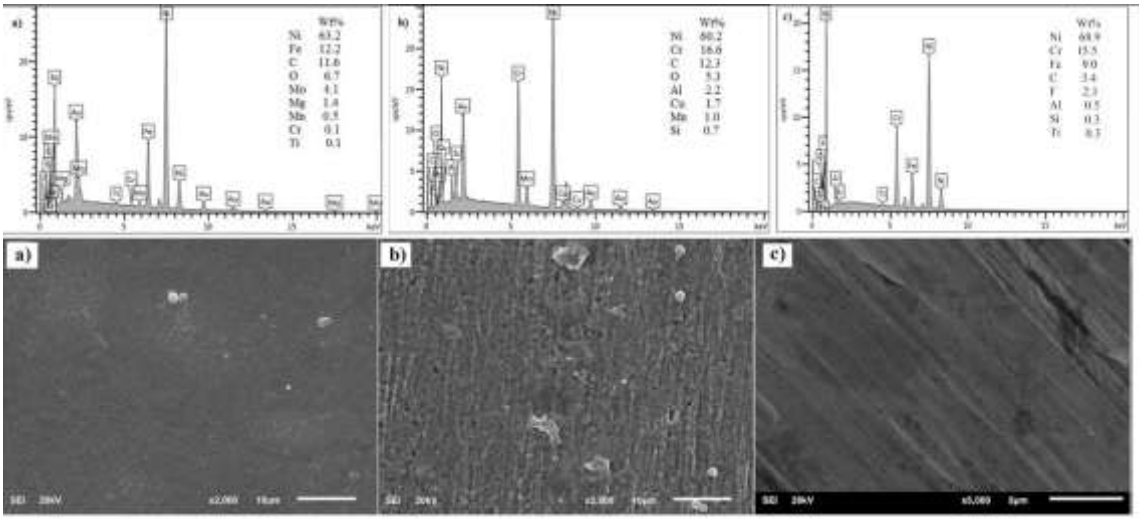

**Figure 4.** EDS and SEM results of a) $Ni_{0.80}Fe_{0.15}Mo_{0.05}$ b) $Ni_{0.75}Cr_{0.20}Al_{0.025}Cu_{0.025}$ and c) $Ni_{0.70}Cr_{0.20}Fe_{0.10}$ alloys recorded at room temperature.

### 3.4. SEM measurements

In SEM experiments, secondary electrons (SE, inelastic scattering) are used for determining sample morphology (topography), back-scattered electrons (BSE, elastic scattering) are important for analayzing sample composition [34]. SEM pictures are recorded at room temperature. In Figure 4, SEM images of two alloys are given. Microstructure properties are seen from micrographs. As shown in SEM figures, for $Ni_{0.80}Fe_{0.15}Mo_{0.05}$, the surface is more smooth than the surface of $Ni_{0.75}Cr_{0.20}Al_{0.025}Cu_{0.025}$. For $Ni_{0.70}Cr_{0.20}Fe_{0.10}$ alloy, the layered surface is seen from SEM picture in Figure 4.

## 4. CONCLUSION

In the present study, 3d transition metal element alloys, $Ni_{0.80}Fe_{0.15}Mo_{0.05,}$ $Ni_{0.70}Cr_{0.20}Fe_{0.10}$ and $Ni_{0.75}Cr_{0.20}Al_{0.025}Cu_{0.025,}$ have been studied by EPR, XRD, EDS and SEM methods at room temperature. From room temperature EPR experiment of $Ni_{0.8}Fe_{0.15}Mo_{0.05}$ alloy, the g values have been calculated as 5.665, 5.333 and 4.396. Due to the fact that the peaks are overlapped we are not able to identificate them clearly. For $Ni_{0.75}Cr_{0.20}Al_{0.025}Cu_{0.025}$ alloy, three lines with g values of 3.719, 2.442 and 2.049 have been observed in the EPR spectrum. EPR parameters obtained for $Ni_{0.70}Cr_{0.20}Fe_{0.10}$ alloy have been given as g = 2.078, 2.026 and 1.934. The lines with g = 2.078 and 1.934 values can not be determined clearly due to the broadness. For all of the alloys, the EPR line properties have given us chance to evaluate the existence of ingredients clearly as supported by the other used techniques. Also by EPR method, we are able to see that these alloys have shown the paramagnetic properties in an applied external magnetic field. In XRD figures, we can observe the position, intensity and sharpness of lines. It is concluded that the difference between line positions and line intensities of samples are because of contents, different proportions of elements and structural properties. The sharpness of XRD peaks have given the crystalline nature of alloys. EDS analysis have shown the elemental composition of the samples which supports the XRD and EPR results. In SEM pictures, microcrystalline properties have been observed. As we have discussed above, from the defined g-values, XRD, EDS, SEM results and the literature knowledge, structural and magnetic properties of these alloys can be understood clearly in the frame of resolution restrictions. Results obtained by EPR experiment show the paramagnetic property of the samples in the presence of an external magnetic field. Also by structural analysis (XRD, SEM, EDS), we have obtain information about the samples with the given alloy ratios for the contribution to the literature.

## REFERENCES

[1]. Yang Y., Wu P., Wang Q., Wu H., Liu Y., Deng Y., Zhou Y., Shuai C. The Enhancement of Mg Corrosion Resistance by Alloying Mn and Laser-Melting. Mater, 9 (2016) 1-10.

[2]. Rodrigues, W.C., Espinoza, F.R.M., Schaeffer, L., Knörnschild, G., A study of Al-Mo powder processing as a possible way to corrosion resistent aluminum-alloys. Mater. Res., 12 (2009) 211-218.

[3]. Han İ., Demir L., Mass attenuation coefficients, effective atomic and electron numbers of Ti and Ni alloys. Radiat. Measure., 44 (2009) 289-294.

[4]. Pervaiz S., Rashid A., Deiab I., Mihai N., Influence of Tool Materials on Machinability of Titanium- and Nickel-Based Alloys: A Review. Mater. Manufacturing Process., 29 (2014) 219-252.

[5]. Davis JR. Nickel, Cobalt, and Their Alloys ASM Specialty Handbook, (2000) 92-101.

[6]. Aygun Z., Aygun M., Karabulut B., Karabulut A., Investigation of non-

irradiated and gamma-irradiated Trommel Sieve Waste (TSW) with EPR technique. Ann. Nucl. Energy, 40 (2012) 84-86.

[7]. Wang H.L., Yan J.M., Li S.J., Zhang X.W., Jiang Q.,. Noble-metal-free NiFeMo nanocatalyst for hydrogen generation from the decomposition of hydrous hydrazine. J. Mater. Chem. A, 3 (2015) 121-124.

[8]. Oleksakova, D., Kollar, P., Fuzer, J., Kusy, M., Roth, S., Polansk, K.,. The influence of mechanical milling on structure and soft magnetic properties of NiFe and NiFeMo alloys. J. Magn. Magn. Mater., 316 (2007) e838-e841.

[9]. Banerjee M., Banerjee, R., Majumdar, A.K., Mookerjee, A., Sanyal, B., Nigam, A.K., Magnetism in NiFeMo disordered alloys: Experiment and theory, Physica B, 405 (2010) 4287-4293.

[10]. Srinivasan R., Sougandi I., Venkatesan R., Rao P.S., Synthesis and room temperature single crystal EPR studies of a dinickel complex having an {Ni2(m-phenoxide)2}2+ unit supported by a macrocyclic ligand environment [Ni2(L)2(OClO3)2] [L = 2-[(4-methyl-pyridin-2-ylimino)- methyl]-phenol]. Proc. Indian Academia Science (Chem. Sci.), 115 (2003) 91-102.

[11]. Manjunatha C., Sunitha D.V., Nagabhushana H., Sharma S.C., Ashoka S., Rao J.L., Nagabhushana B.M., Chakradhar R.P.S., Structural characterization, EPR and thermoluminescence properties of Cd1-xNixSiO3 nanocrystalline phosphors. Mater. Res. Bulletin, 47 (2012) 2306-2314.

[12]. Aygun Z., Aygun M., Spectroscopic analysis of Ahlat stone (ignimbrite) and pumice formed by volcanic activity. Spectrochim. Acta A, 166 (2016) 73–78.

[13]. Reddy A.J., Kokila M.K., Nagabhushana H., Chakradhar R.P.S., Shivakumara C., Rao J.L., Nagabhushana B.M.,Structural, optical and EPR studies on ZnO:Cu nanopowders prepared via low temperature solution combustion synthesis. J. Alloy Comp., 509 (2011) 5349-5355.

[14]. Li, Y., Fu, Q., Flytzani-Stephanopoulos, M. Low-temperature water-gas shift reaction over Cu- and Ni-loaded cerium oxide catalysts. Appl. Catalysis B: Environ, 27 (2001) 179-191.

[15]. Kabir L., Mandal A.R., Mandal S.K., Polymer stabilized Ni–Ag and Ni–Fe alloy nanoclusters: Structural and magnetic properties. J. Magn. Magn. Mater, 322 (2010) 934-939.

[16]. Yarbasi Z., Karabulut A., Karabulut B. EPR Studies of Copper-Doped Potassium Dihydrogen Citrate ($C_6H_7KO_7$) Single Crystal. Appl. Magn. Resonance, 41 (2011) 51-57.

[17]. Stucki J.W., Banwart W.L. Advanced chemical Methods for Soil and Clay Minerals Research; ed. Reidel Pub; 1980.

[18]. Mcbride M.B., Electron Spin Resonance spectroscopy In Instrumental Surface Analysis of Geologic Materials; ed. Perry DL VCH, Newyork; 1990.

[19]. Slater, A.F.G., Swıggard, W.J., Orton, B.R., Flıtter, W.D., Goldberg, D.E., Ceramı, A., Henderson, G.B.,. An iron-carboxylate bond links the heme units of malaria pigment. Proc. National Academic Sci., 88 (1991) 325-329.

[20]. Walker, F.A., Huynh, B.H., Scheidt, W.R., Osvath, S.R., Models of the Cytochromes b. Effect of Axial Ligand Plane Orientation on the EPR and Mb'ssbauer Spectra of Low-Spin Ferrihemes. J. American Chem. Soc., 108 (1986) 5288-5297.

[21]. Fujii, H., Yoshimura, T., Kamada, H., ESR Studies of A1u and A2u Oxoiron(IV) Porphyrin ð-Cation Radical Complexes. Spin Coupling between Ferryl Iron and A1u/A2u Orbitals. Inorganic Chem., 35 (1996) 2373-2377.

[22]. Davis, L.C., Henzl, M.T., Burris, R.H., Orme-Johnson, W.H., Iron-Sulfur Clusters in the Molybdenum-Iron Protein

Component of Nitrogenase. Electron Paramagnetic Resonance of the Carbon Monoxide Inhibited State. Biochem. 1 (1979) 4860-4869.

[23]. Fedorov V.V., Konak T., Dashdorj J., Zvanut, M.E., Mirov S.B. Optical and EPR spectroscopy of Zn:Cr:ZnSe and Zn:Fe:ZnSe crystals. Opt. Mater.,37 (2014) 262-266.

[24]. Vercamer V., Lelong G., Hijiya H., Kondo Y., Galoisy L., Calas G., Diluted $Fe^{3+}$ in silicate glasses: Structural effects of Fe-redox state and matrix composition. An optical absorption and X-band/Q-band EPR study. J. Non-Cryst. Solids, 428 (2015) 138-145.

[25]. PushpaManjari V., Aswani T., Babu B., Thirumala Rao G., Joyce Stella R., Jayaraja B., Ravikumar R.V.S.S.N. EPR and Optical Studies of Cr (III) Ions Doped NaCaAlPO4F3 Nano Phosphor. Inter. J. Current Eng. Technol., 2 (2004) 259-264.

[26]. Padlyak B.V., Romanowski W.R., Lisiecki R., Adamiv V.T., Burak Y.V., Teslyuk I.M., Synthesis, EPR and optical spectroscopy of the Cr-doped tetraborate glasses. Opt. Mater.,34 (2002) 2112-2119.

[27]. Alıahmad, M., Moghaddam, N.N. Synthesis of maghemite (g-Fe2O3) nanoparticles by thermal-decomposition of magnetite (Fe3O4) nanoparticles. Mater. Sci. Poland , 31 (2013) 264-268.

[28]. Drbohlavova J., Hrdy R., Adam V., Kizek R., Schneeweiss O., Hubalek J. Preparation and Properties of Various Magnetic Nanoparticles. Sensors, 9 (2009) 2352-2362.

[29]. Iwasaki, T., Mechanochemical Synthesis of Magnetite/Hydroxyapatite Nanocomposites for Hyperthermia. Mater. Sci.-Advanced Topics, 8 (2013) 175-194.

[30]. Ul-Hamid, A., Quddus, A., Saricimen, H., Dafall, H., Corrosion Behavior of Coarse- and Fine-Grain Ni Coatings Incorporating NaH2PO4.H2O Inhibitor Treated Substrates. Mater. Res., 18 (2015) 20-26.

[31]. Anđić, Z., Vujović, A., Tasić, M., Korać, M., Kamberovic, Z., Synthesis and characterization of Dispersion Reinforced Sintered System Based on Ultra Fine and Nanocomposite Cu-Al2O3 Powders. Dr. Yoshitake Masuda (Ed.), (2011) 217-236.

[32]. Saravanan, G., Mohan, S., Electrodeposition of Fe-Ni-Cr alloy from Deep Eutectic System containing Choline chloride and Ethylene Glycol. Int. J. Electrochem. Sci., 6 (2011) 1468-1478.

[33]. Park, J.H., Kim, H.G., Park, J.Y., Jung, Y.I., Park, D.J., Koo, Y.H., 2015. High temperature steam-oxidation behavior of arc ion plated Cr coatings for accident tolerant fuel claddings. Surface & Coatings Technol., 280 (2015) 256-259.

[34]. Aygun, Z., 2013. AFM and SEM Studies of $VO^{2+}$ Doped Potassium Dihydrogen Citrate Single Crystal Obtained by Slow Evaporation Method. J. Chem. Crystallog., 43 (2013) 103-107.